# Novel Dual Marx Generator for Microplasma Applications

Tammo Heeren, *Member, IEEE*, Takahisa Ueno, Douyan Wang, *Member, IEEE*, Takao Namihira, *Member, IEEE*, Sunao Katsuki, *Member, IEEE*, and Hidenori Akiyama, *Fellow, IEEE*

*Abstract*—Micrometer size plasmas, or microplasmas, find applications in pollution control, reduction, and prevention. The required nonthermal plasmas can be generated by either an electron beam or an electric discharge. The pulse widths and voltages necessary to generate these nonthermal plasmas are $10^{-10}$–$10^{-8}$ s, and $10^3$–$10^4$ V, respectively, depending on the application. The required energy is typically in the low $10^{-3}$ J range. This paper presents a novel circuit design to generate high-voltage pulses with variable pulse widths and pulse rise and fall times in the low $10^{-9}$ s regime. The circuit employs two parallel Marx Generators utilizing bipolar junction transistors (BJTs) as closing switches. The BJTs are operated in the avalanche mode to yield fast rise times. The design allows for positive or negative polarity pulses, and can easily be changed to yield higher or lower output voltage.

*Index Terms*—Avalanche breakdown, Marx generators, plasma generation, pulse generation.

## I. INTRODUCTION

IN most industrialized countries air pollution due to conversion of energy from fossil fuels is of great concern. Especially the removal of $NO_x$ and $SO_x$ is of major interest. The application of nonthermal plasmas suggests an energy-efficient way to remove these pollutants [1]. These nonthermal plasmas can be created either by electron beam irradiation or an electrical discharge. The employment of pulsed power to produce these electrical discharges rather than electron beam irradiation is attractive due to various reasons such as reduced equipment cost, absence of X-ray radiation, and insignificant heating [2]. A number of factors have influence on the energy efficiency of the process. These factors are, among others [2], include voltage polarity, peak voltage, pulse width, and pulse repetition rate. Various reactors, such as wire-to-plate reactors [3], coaxial reactors [4], cylindrical wire-to-mesh reactors [5], and others [1] have been used. The pulsed power generators that are used to energize these systems are magnetic pulse compressors [3] and multistage Blumlein lines [4]. Other pulse generators that could be used are the Marx-generator or a charged-line pulser. It is suggested [2], [6] that shorter pulsewidth and a supercritical fluid environment (high gravity, high pressure) significantly improves removal efficiency of the $NO_x$ and $SO_x$. This imposes a number of restrictions on the pulse power generator, such as the following: significantly smaller rise and fall time (to allow
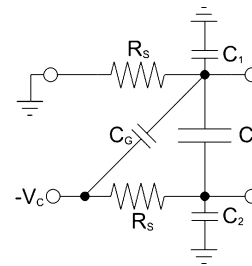
Fig. 1. Representation of a single Marx generator stage after the previous stage has fired. $C_1$ and $C_2$ are stray capacitances. $R_S$ and $C_S$ are stage resistance and capacitance.

for short pulse width); more compact design such that the parasitic inductance can be minimized (to minimize pulse rise and fall times); possibility to change polarity, peak voltage, pulse width, and repetition rate.

None of the above mentioned pulse generators fulfill all of these criteria, but the Marx generator has some unique properties that might make it an ideal candidate.

## II. PULSE WIDTH PROBLEM

Though Marx generators can provide superior rise time, the pulsewidth can become a problem. The Marx generator, while discharging, can be approximated as a simple capacitor $C_E$ with a parallel resistance $R_E$. If a conventional generator design is assumed, then

$$C_E = \frac{C_S}{n} \text{ and } R_E = \frac{n+1}{2} \cdot R_S \qquad (1)$$

where $C_S$ and $R_S$ are the stage capacitance and resistance, respectively, and $n$ is the number of stages. If it is also assumed that $R_E \gg R_L$, the load resistance, then the discharge is a resistance-capacitance ($RC$ discharge dominated by the time-constant $\tau = C_E R_L$. The time for the voltage to drop to a certain level $x$ (in percentage of the charging voltage) is given by

$$t(x) = -\ln(x) \cdot R_E \cdot C_E. \qquad (2)$$

To reduce the pulse width, the stage capacitance $C_S$ could simply be reduced until $t(x)$ results in an acceptable value. This might work for larger Marx generators with pulse widths in the microsecond range, but for pulse widths in the nanosecond regime, this leads to unexpected problems. Expanding on Pai's discussion [7] of the approximate representation of a single Marx generator state (see Fig. 1), it is obvious that for overvoltage triggered switches, certain conditions have to be
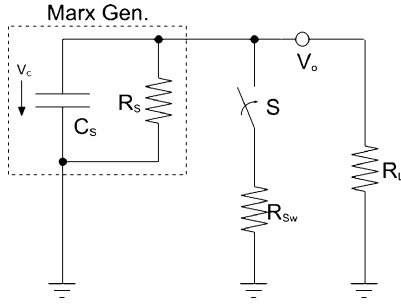
Fig. 2. Equivalent circuit for a Marx generator with an additional closing switch to connect the output through switch resistance $R_{Sw}$ to ground.
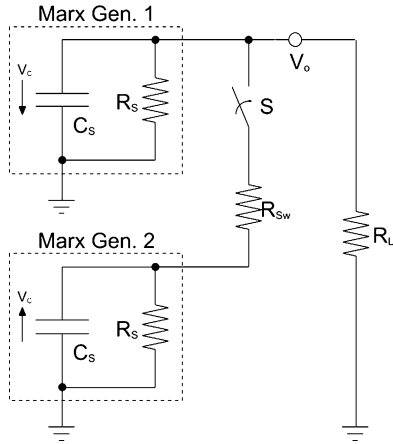


Fig. 3. Equivalent circuit for a Marx generator with an additional closing switch to connect the output through switch resistance $R_{Sw}$ to ground.

met. Including the stage capacitance $C_S$ in the equation for the voltage across the switch [7] results in

$$V_s = 1 + \frac{C_{S,2} + C_1}{C_{S,2} + C_1 + C_G}, \text{ where } C_{S,2} = \frac{C_S \cdot C_2}{C_S + C_2}. \quad (3)$$

Only if $C_{S,2} + C_1$ is much larger than $C_G$ (factor 10–100) will a sufficient overvoltage condition take place. Since $C_2$ is the main energy storage device, it should, by itself, be approximately 10–100 times larger than the stray capacitances. Otherwise a large portion of the stored energy is deposited into the stray capacitances and not available for the actual discharge through the load. Thus, the stage capacitance $C_S$ should be about $10^2$–$10^4$ times larger than the switch capacitance $C_G$. This problem is somewhat alleviated by the number of stages in a Marx generator, since $C_S = n \cdot C_E$.

Instead of reducing the pulse width by reducing the stage capacitance, an additional switch could be used to pull the output to ground. The benefit is that the stage capacitance can be sufficiently large to provide an almost flat top pulse. If the circuit in Fig. 2 is considered, the voltage $V_o$ at the output of the circuit falls with a time-constant of $\tau = R_S \| R_{Sw} \| R_L \cdot C_S$. Assuming that $R_L \| R_S \gg R_{Sw}$, then the fall time is dominated by the switch resistance and is largely independent of the closing speed of the switch.

The circuit shown in Fig. 3 depicts two counter pulsing Marx generators, isolated by an overvoltage triggered closing switch. If it as again assumed that $R_S \| R_L \gg R_{Sw}$ then, at the time of switching $t_1$, both voltages from the Marx Generators 1 and 2
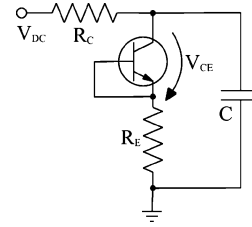


Fig. 4. Overvoltage breakdown test circuit ($R_C = 68\,\text{k}\Omega$, $C = 1\,\text{nF}$, $R_E = 2\ldots200\,\Omega$, BJT = ZETEX417).

will compensate each other (assuming $C_S \cdot R_S \| R_L \gg t_1$) and the voltage $V_o$ will be (almost) at ground potential. The residual voltage will decay with a time constant of $\tau = C_S/2R_{Sw}$. However, the initial fall time is half of that of the previous example and dependent on the closing speed of the switch $S$ and less on the switch resistance.

## III. AVALANCHE BREAKDOWN

The application of semiconductor switches to Marx generators is beneficial from many points of view, some of which are compactness, reliability, lifetime, and stability of the switching action. Two major drawbacks are that most devices need to be triggered externally, which adds to the complexity of the design, and that the switching speed is limited by the drift velocity of the charge carriers for the particular device [8]. These two drawbacks can be eliminated if the semiconductor switch can be operated in the avalanche mode. In the avalanche mode the switch is operated at a voltage that is close to the breakdown voltage of its reversed biased PN junction. If the voltage exceeds this limit, impact ionization and carrier multiplication will lead to an avalanche breakdown of the junction [9]. Since new carriers are generated within the junction itself, the switching time is effectively reduced by the rate the new carriers are created, e.g., by the ionization rate. This can lead to switching time constants in the $10^{-12}$ s range [8].

## IV. PULSE RISE TIME LIMITATIONS

To investigate the performance of the specialized ZETEX417 Avalanche Transistor during the over-voltage breakdown transition, the circuit shown in Fig. 4 is employed. It allows the measurement of the breakdown voltage $V_{BD}$, the determination of the switching speed as a function of the peak current $I_{max}$, and of the emitter resistance $R_E$. Whereas the breakdown voltage $V_{BD}$ showed no significant dependence on the emitter resistance, the 10%–90% current rise time $t_R$ is very well dependent on it. To determine the device impedance, the peak device current $I_{S\,max}$ is plotted in Fig. 5 as a function of emitter conductance $1/R_E$. With decreasing $R_E$, the curve deviates from the ideal straight line, and the deviation can be attributed to the impedance of the device. However, since the peak current coincides with $dI/dt = 0$, there is no inductive voltage drop and the additional impedance can solely be attributed to the device and not to any stray inductance in the system. In our case, the device impedance is about $R_S = 3\,\Omega$.

The 10%–90% current rise time $t_R$ as a function of emitter resistance is plotted in Fig. 6. Obviously, it is dependent on the emitter resistance with about 10 ps/$\Omega$. In addition, Fig. 6 also
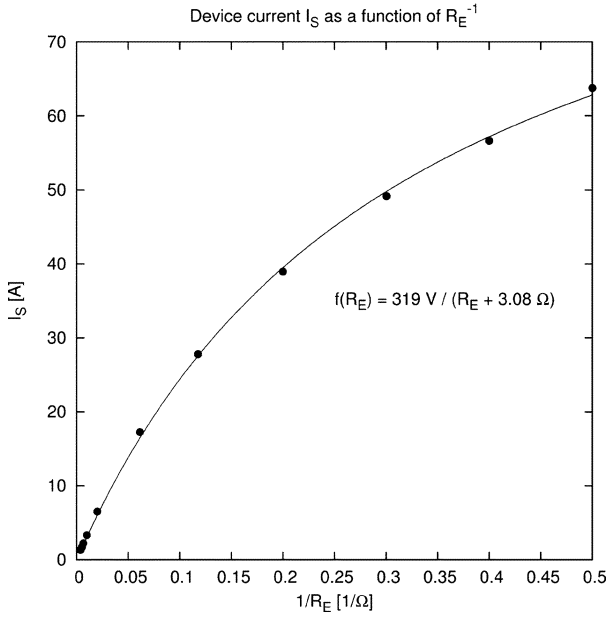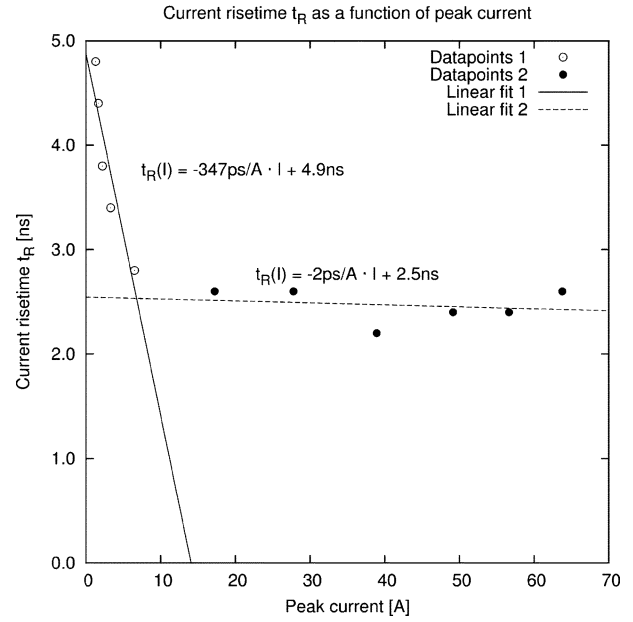
Fig. 5.   Peak device current $I_{S\,\max}$ as a function of emitter conductance $1/R_E$.



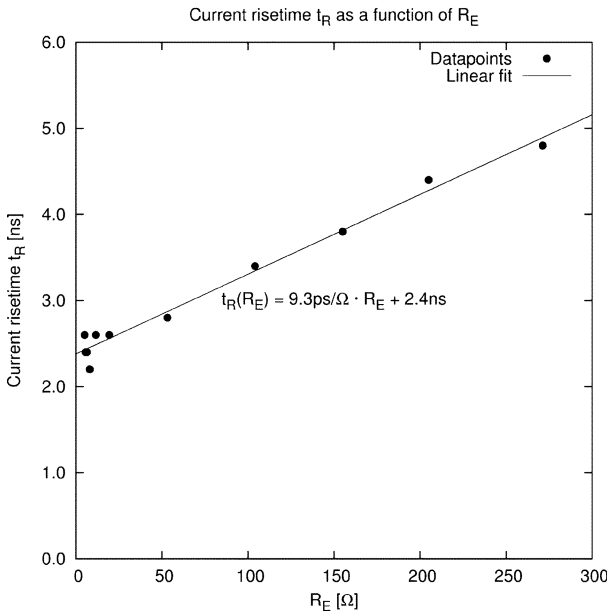Fig. 7.   10%–90% current rise time as a function of peak current.



Fig. 6.   10%–90% current rise time as a function of emitter resistance.
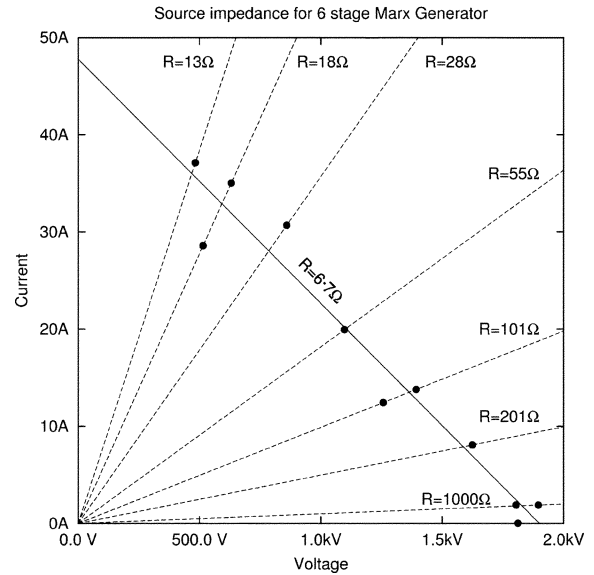


Fig. 8.   Measurements of load current versus load voltage (dashed lines), load impedance for variable loads (solid line), and source impedance lines (circles).

illustrates that the rise time is not dominated by the inductance of this circuit, but by the device (at least for rise times greater 2.5 ns). In any resistance-capacitance-inductor *RLC* circuit, the current rise time is inversely proportional to the circuit resistance, independent of whether the circuit is over, under, or critically damped. This is obviously not the case here. Assuming $t_R = 2.5$ ns, $R_E = 20\ \Omega$, and $C = 1$ nF, the inductance of the circuit can not be larger than $L \approx 14$ nH.

Fig. 7 shows the 10%–90% current rise time $t_R$ as a function of peak current ($\sim 1/RE$). Above approximately 10 A ($\sim 30\ \Omega$), the rise time is almost independent of the peak current, which we think is due to the rise time limitation of the oscilloscope used in the measurements.

## V. PROTOTYPE EVALUATION

To prove the feasibility of the switching concept illustrated in Fig. 3 and to evaluate its potential performance a six-stage dual Marx Generator shown in Fig. 11, with the conceptual schematic in Fig. 12, was built and tested. All components are surface mounted devices (SMD), besides the artificial stray capacitances. The stage capacitance is 1 nF and the stage voltage is approximately 320 V. The impedance of one Marx Generator was determined by measuring the voltage across a variable resistive load. By plotting output current over output voltage, we found the total source impedance to be approximately 42 $\Omega$ for a six-stage Marx Generator ($\sim 7\ \Omega$ per stage). Detailed results are shown in Fig. 8. The energy deposition into the load as a
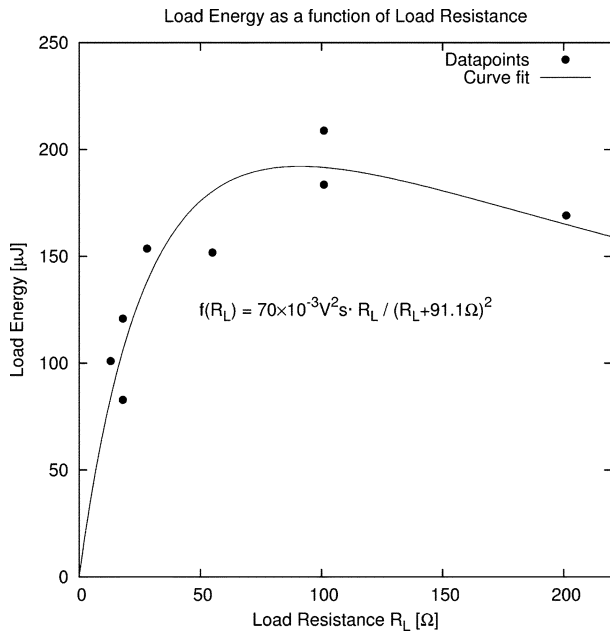
Fig. 9. Measurements of energy deposited into load as a function of load resistance (solid line) and least square fit (circles).
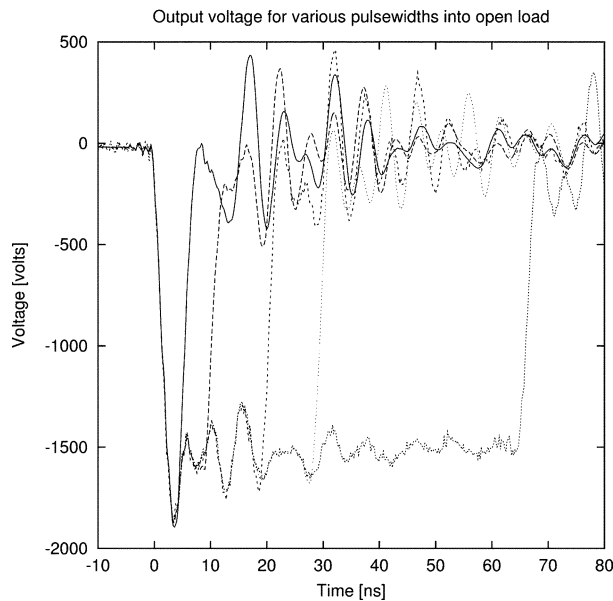


Fig. 10. Output voltage for various pulse-widths into open load of the prototype dual Marx generator.

function of load resistance $R_L$ is shown in Fig. 9. The peak energy is in the range of 150–200 $\mu$J, with an energy stored in the Marx Generator in the range of 300–400 $\mu$J.

The initial idea of counter-pulsing two independent Marx Generators with opposite polarities was tested with the same prototype, as shown in Fig. 11. Each generator is capable of producing 1.5–1.8 kV; the top generator with negative polarity and the bottom generator with positive polarity. Each of them are triggered individually from a secondary driver board. The output pulse width $T_{pw}$ is adjusted by delaying the triggering of one Marx Generator by $\Delta t = T_{pw}$. If the top (negative) Marx is triggered first, a negative pulse is delivered to a load connected to the top Marx. If the bottom one is triggered first, a positive
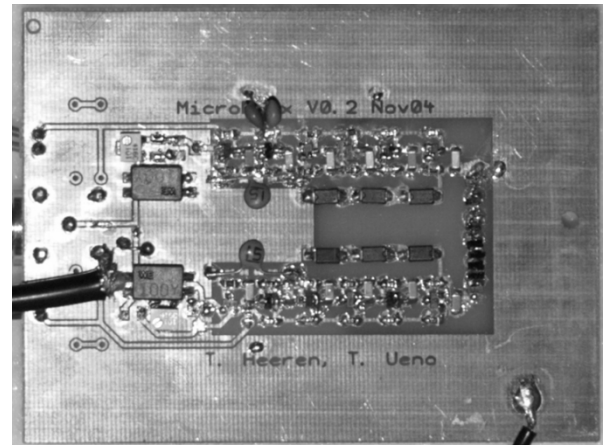


Fig. 11. Prototype six-stage dual Marx generator (7 cm × 10 cm). Some of the switches that isolate both generators have been removed to test each generator individually. It also shows the addition of artificial "stray" capacitors to support the proper erection of the generators.
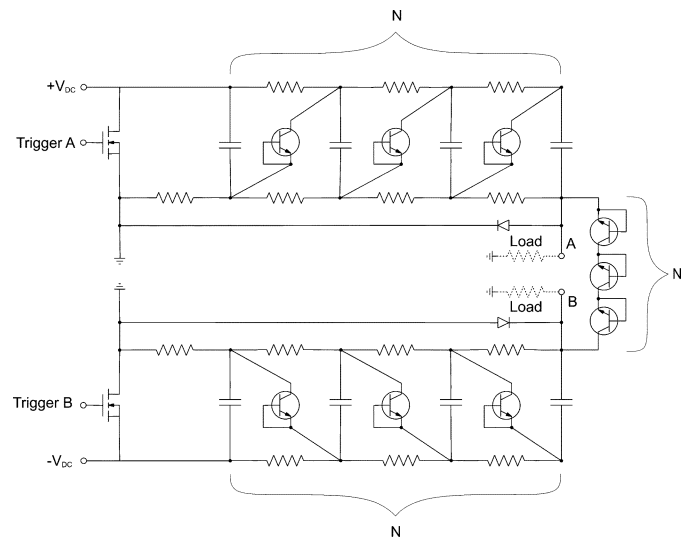


Fig. 12. Conceptual schematic of a three stage dual Marx generator. Number of stages $N$ can be increased to yield higher voltages. Load can either be connected to point A or point B, depending on the desired polarity.

pulse is delivered to a load connected to the bottom Marx. A set of measurements for various pulsewidths and negative polarity is shown in Fig. 10. The measurements where done into open load show the large range in which the pulse width can be varied. For loads smaller than the impedance of the charging network ($\sim N \cdot R_S/2$), the pulsewidth is mainly limited by the $RC$ time-constant and larger capacitors might be required to limit the voltage drop during the pulse.

## VI. SUMMARY AND CONCLUSION

A prototype of a novel dual Marx generator suitable of delivering kV pulses with rise and fall times in the low nanoseconds regime was built and tested. The design is flexible to allow for changes in pulse width, polarity, and peak voltage of the output pulse. The generator was successfully miniaturized by utilizing surface mount devices. The individual switches were characterized with regard to impedance and current dependent switching time. It was found that the over-voltage breakdown took place

at about 320 V, that the switch impedance was roughly 3 $\Omega$, and that the switching speed was inversely proportional to the current. The individual Marx Generators were analyzed and it was found that each stage had an equivalent source impedance of approximately 7 $\Omega$. The initial idea of two counter-pulsing generators to achieve fast rise and fall times was successfully tested and the ability to adjust the pulse width from 4 to 60 ns while keeping the rise and fall times in the low 2-ns regime was shown.

Applications of this technology are not only in the generation of micron-sized plasmas, but also in the newly emerging field of bioelectrics where cells are exposed to high, short duration, electric fields. Other areas of applications can be the generation of repetitive high-voltage trigger pulses for high speed cameras and spectrometers.

## REFERENCES

[1] R. Hackam and H. Akiyama, "Air pollution control by electric discharges," *IEEE Trans. Dielectr. Electr. Insul.*, vol. 7, no. 5, pp. 654–683, Oct. 2000.

[2] ——, "Application of pulsed power for the removal of nitrogen oxides from polluted air," *IEEE Electr. Insul. Mag.*, vol. 17, no. 5, pp. 8–13, Sep./Oct. 2001.

[3] D. Wang, T. Namihira, K. Fujiya, S. Katsuki, and H. Akiyama, "The reactor design for diesel exhaust control using a magnetic pulse compressor," *IEEE Trans. Plasma Sci.*, vol. 32, no. 5, pp. 2038–2044, Oct. 2004.

[4] T. Namihira, S. Tsukamoto, D. Wang, S. Katsuki, R. Hakam, H. Akiyama, Y. Uchida, and M. Koike, "Improvement of $NO_x$ removal efficiency using short-width pulse power," *IEEE Trans. Plasma Sci.*, vol. 28, no. 2, pp. 434–442, Apr. 2000.

[5] S. Tsukamoto, T. Namihira, D. Wang, S. Katsuki, R. Hakam, H. Akiyama, A. Sato, Y. Uchida, and M. Koike, "Effects of fly ash on $NO_x$ removal by pulsed streamers," *IEEE Trans. Plasma Sci.*, vol. 29, no. 1, Feb. 2001.

[6] E. Lock, A. Saveliev, and L. A. Kennedy, "Application of nonthermal plasma for pollution control in a supercritical fluid environment," presented at the Proc. AIChE Annu. Meeting, San Francisco, CA, Nov. 16–21, 2003.

[7] S. T. Pai and Q. Zhang, *Introduction to High Power Pulse Technology*, Singapore: World Scientific, 1995, ch. 2.3.

[8] Y. Mizushima and Y. Okamoto, "Properties of avalanche injection and its application to fast pulse generation and switching," *IEEE Trans. Electron Devices*, vol. Ed-14, no. 3, pp. 146–157, Mar. 1967.

[9] B. G. Streetman and S. Banerjee, *Solid State Electronic Devices*. Englewood Cliffs, NJ: Prentice Hall, 2000, ch. 5.4.

**Takahisa Ueno** was born in Oita, Japan, on August 4, 1982. He received the B.S. degree in 2005 from Kumamoto University, Kumamoto, Japan, where he is currently working toward the M.S. degree.

**Douyan Wang** (M'04) was born in Beijing, China, on May 18, 1975. She received the B.S., M.S. and Ph.D. degrees from Kumamoto University, Kumamoto, Japan, in 1998, 2000, and 2005 respectively.

She is currently a Research Associate with the 21st Century Center of Excellence (COE) Program, Kumamoto University. From 2000 to 2002, she was with Hitachi, Ltd., Ibaraki, Japan. From November 2003 to March 2004, she was on sabbatical leave at the Center for Pulsed Power and Power Electronics, Texas Tech University, Lubbock.

Dr. Wang was a Japan Society for the Promotion of Science (JSPS) Research Fellow during 2003–2005.

**Takao Namihira** (M'00) was born in Shizuoka, Japan, on January 23, 1975. He received the B.S., M.S., and Ph.D. degrees from Kumamoto University, Kumamoto, Japan, in 1997, 1999, and 2003, respectively.

Since 1999, he has been a Research Associate at Kumamoto University. He was on sabbatical leave at the Center for Pulsed Power and Power Electronics, Texas Tech University, Lubbock.

**Sunao Katsuki** (M'99) was born in Kumamoto, Japan, on January 5, 1966. He received the B.S., M.S., and Ph.D. degrees from Kumamoto University, Kumamoto, Japan, in 1989, 1991, and 1998 respectively.

From 1991 to 1998, he was a Research Associate at Kumamoto University, where he is currently an Associate Professor. During 2001–2002, he was a Senior Researcher at the Plasma and Electronics Research Institute (PERI), Old Dominion University, Norfolk, VA.

**Tammo Heeren** (M'00) was born in Oldenburg, Germany, on January 16, 1972. He received the B.S. degree from the University of Applied Science, Wilhelmshaven, Germany, in 1998. He received the M.S.E.E and Ph.D. degrees from Texas Tech University, Lubbock, in 2000 and 2003, respectively.

He joined the Center for Pulsed Power and Power Electronics, Texas Tech University, Lubbock, as a Senior Research Assistant. From 2004 to 2005, he was a Visiting Associate Professor at Kumamoto University, Kumamoto, Japan, and is now Visiting Faculty at the Center for Bioelectrics, Old Dominion University, Norfolk, VA.

**Hidenori Akiyama** (M'87–SM'99–F'00) received the Ph.D. degree from Nagoya University, Nagoya, Japan, in 1979.

From 1979 to 1985, he was a Research Associate at Nagoya University. In 1985, he joined the faculty at Kumamoto University, Kumamoto, Japan, where he is currently a Professor.

Dr. Akiyama received the IEEE Major Education Innovation Award in 2000 and the IEEE Peter Haas Award in 2003.